

# INVESTIGATION OF THE ENERGY-HEIGHT RELATION FOR SOLAR FLARE FOOTPOINTS OBSERVED BY *RHESSI*

T. Mrozek and J. Kowalczyk

*Astronomical Institute, University of Wrocław,  
ul. Kopernika 11, 51-622 Wrocław, Poland*

**Abstract.** Footpoints of several solar flares have been investigated using RHESSI images. We measured the altitude of hard X-ray footpoint sources above the photosphere. The relation between the height and the energy of sources was studied. Some observational characteristics of the energy-height relation have been obtained. Using them we were able to conclude that during an impulsive phase the region in which electrons are stopped is rather narrow with the thickness in the range 1000–5000 km. Moreover, the obtained relations were used for reconstruction of the density structure in the collision region.

**Key words:** solar flares - footpoints - hard X-rays

## 1. Introduction

During a solar flare energy stored in a magnetic field is converted into other types of energy. About half of that energy goes into energetic particles. Accelerated particles propagate outward to interplanetary space and downward to a dense chromosphere. Due to Coulomb collisions with ambient plasma they lose energy that is consumed for heating the chromosphere and for emission of bremsstrahlung photons. As a product of this scenario we observe emission sources, visible in wide range of wavelengths, located close to or in the chromosphere - solar flare footpoints.

The depth that can be reached by an energetic particle is related to the column density along the path of that particle. As a consequence an electron with larger initial energy can penetrate deeper into the chromosphere than an electron with smaller initial energy. Roughly speaking the energy of a non-thermal electron is related to the energy of the HXR photon emitted during collision. Thus a relation between the energy of hard X-ray footpoint

sources and their positions along the flux tube, i.e. the energy-height relation should be observed (Brown & McClymont 1975).

Matsushita et al. (1992) analyzed heights of HXR sources measured in *YOHKOH*/HXT four energy channels: 14-24 keV (L), 24-34 keV (M1), 34-54 keV (M2) and 54-94 keV (H). They compared the location of HXR sources to H $\alpha$  flare position taken from the *Solar-Geophysical Data*. The position of the H $\alpha$  flare was treated as a reference level of the base of the chromosphere. Average heights of HXR sources determined in four energy channels were as follows:  $9.7 \pm 2.0$  Mm (L),  $8.7 \pm 0.3$  Mm (M1),  $7.7 \pm 0.5$  Mm (M2)  $6.5 \pm 0.7$  Mm (H).

The first attempt to study the energy-height relation for HXR footpoint sources with the use of *RHESSI* (Lin et al. 2002) data was made for one flare by Aschwanden et al. (2002). HXR footpoint sources were observed at heights that were of almost 7 Mm smaller than that obtained by Matsushita et al. (1992). This large inconsistency was explained as a result of systematical error in an analysis made by Matsushita et al. (1992) caused by the H $\alpha$  flare position. The authors showed that the excellent energy resolution of *RHESSI* data gives opportunity for detailed analysis of the energy-height relation, which may be useful in analysing the density structure. Mrozek (2006) made an attempt to a statistical analysis of the relation and obtained the average heights of HXR footpoint sources similar to the ones got by Aschwanden et al. (2002). Moreover it was shown that the relation observed with *RHESSI* data is sensitive to very small changes of the density thus, gives opportunity for a detailed investigation of the chromospheric evaporation at several levels of the chromosphere.

The investigation made by Mrozek (2006) included several flares observed by *RHESSI* during the first two years of operation. In this paper we extend this analysis another flares chosen from observations made between February 2004 and February 2006.

## 2. Observations and Analysis

Among a number of flares observed by *RHESSI* from February 2004 to February 2006 we selected events located close to the solar limb (radial distance greater than  $800''$ ) for which the entire impulsive phase was observed. From this group we selected flares in which sources showing the energy-height relation had been found during a prompt inspection of *RHESSI* im-

**Table I:** List of analyzed flares. (1) - Date, (2) - Beginning of the flare in 12-25 keV range, (3) - GOES class, (4) - Heliographic coordinates, (5) - Distance from the solar disc center["].

Lp.	(1)	(2)	(3)	(4)	(5)
1	06 III 2004	12:11:56	M 1.3	S15E89	987
2	18 III 2004	06:00:40	C 3.7	N15E89	972
3	17 V 2004	04:13:52	C 7.0	S07W85	943
4	17 VII 2004	19:16:20	C 5.3	N07E85	943
5	12 IX 2004	18:29:52	C 2.0	S09W68	885
6	01 XI 2004	06:57:44	C 2.9	N12W83	941
7	23 XI 2004	15:04:24	C 6.5	S06E89	989
8	21 I 2005	00:21:08	C 5.8	N17W74	915
9	21 I 2005	10:12:56	M 1.7	N19W89	961
10	05 V 2005	20:11:16	C 7.8	S06W64	857
11	09 V 2005	18:44:44	B 9.7	N14E64	860
12	30 VII 2005	06:27:44	X 1.3	N08E59	822
13	22 VIII 2005	17:01:20	M 5.6	S16W64	865
14	08 IX 2005	16:54:52	M 2.1	S14E89	948
15	19 IX 2005	16:39:16	B 3.2	S12,W77	925

ages made in relatively wide (few keV) energy intervals. In total, we selected 15 events that are presented in Table I.

In each flare under study at least one strong HXR burst was observed during an impulsive phase. For each HXR burst we have chosen a time interval covering the burst and we have reconstructed a set of images in different energy ranges. The energy ranges have different widths ranging from 2 keV to 20 keV in dependence of counts statistic. Each subsequent energy interval was shifted with regard to the former one by a half of the width of the energy bins. This gave us energy ranges that have small influence from neighboring intervals and can be treated as almost independent. Images were reconstructed using the CLEAN algorithm (Högbom, 1974, Hurford et al. 2002), which is fast and gives best estimation of source location. We used grids Nos. 3-6,8 and 9. This combination gives spatial resolution of the order of 9" and allows to determine the centroid location with accuracy better than 1". The imaging parameters for different energy intervals are

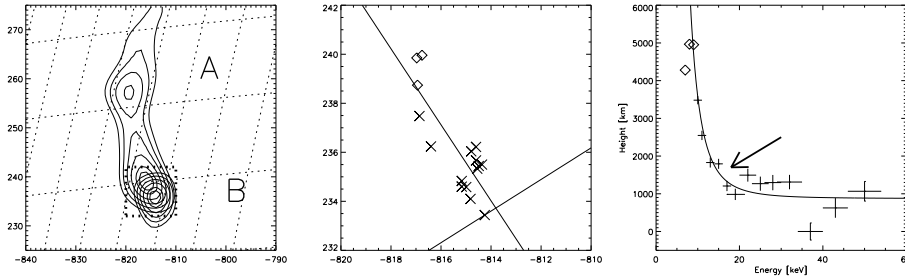


Figure 1: 9 May 2005 flare. Left panel: contours of the emission observed in two ranges: 8-10 keV and 62-82 keV. Dotted box marks the region presented in the middle panel. Middle panel: centroids location for the source B from left panel. Linear fit to these points and reference level are presented. See text for more details. Right panel: altitudes of centroid above reference level; power-law fit is shown with solid line; an approximate location of flattening point is marked with an arrow. Points dominated by thermal emission are marked with diamonds. They were not used for fitting.

identical, i.e. they do not affect the relative positions of centroids.

The set of images obtained in different energy ranges has been used for the further analysis. For each footpoint we draw a map of its centroids obtained in different energies and we fitted a straight line (Fig. 1, middle panel). Next, we defined a reference level as a line perpendicular to the fit and passing by a centroid obtained for the highest energy. For each footpoint we measured its distance from the reference level.

Usually, a strong correlation between a hard X-ray source altitude above the defined level and its energy has been observed. Centroids of high-energy sources were located systematically lower in the chromosphere than the low-energy ones. An example of such behavior is presented in Fig. 1 (right panel). Horizontal lines represent the energy intervals. Errors in the centroid location were calculated using method proposed by Bogachev et al. (2005). The method gives good error estimation for *RHESSI* data in the case of compact and bright sources and cannot be used for large and weak structures. Using these errors we were able to calculate errors in the height estimation. These values are presented as vertical lines.

Moreover, in Fig. 1 (right panel) we present an example of a power-law function fitted to the observed relation. We tested other types of analytic functions (hyperbolic, logarithmic etc.), but found no significant differences.

In the further analysis we used power-law fit because it could be easily inverted for obtaining the density distribution (Brown et al. 2002; Aschwanden et al. 2002). Assuming a zero pitch angle and neglecting pitch angle scattering we can define a column density  $N$  needed to stop an electron of energy  $E$ :

$$N(E) = \frac{E^2}{2K} \quad (1)$$

where  $K$  is a constant (Spitzer 1962). In the simplest case we assume that electrons of energy  $E$  produce (via collisions) photons of energy  $\epsilon \approx E$ . Thus, having from observations a relation between the photon energy of a source ( $\epsilon$ ) and its altitude ( $z$ ):

$$z(\epsilon) = z_0 \left( \frac{\epsilon}{20 \text{ keV}} \right)^{-a} \quad (2)$$

we can obtain from Eq. 1 a column density related to depth in the solar atmosphere. Finally, derivating  $N$  with regard to  $z$  we get the relation between the number density ( $n$ ) and depth:

$$n(z) = n_0 \left( \frac{z}{z_0} \right)^{-1+\frac{2}{a}} \quad (3)$$

It should be noted that this method gives estimation for total neutral and ionized hydrogen density.

From observations we are able to measure the altitude of non-thermal HXR sources measured above arbitrary chosen reference level and calculate a density distribution. Next, we can use the density-height relation obtained from observations for calculating the photospheric altitude. Namely, with Eq. 3 we can calculate an altitude corresponding to a density equal to  $1.16 \times 10^{17} \text{ cm}^{-3}$  (density of the base of the photosphere). Thus, the previously assumed reference level can be corrected and an altitude of observed HXR sources can be related directly to the solar atmosphere.

According to Mrozek (2006) the power-law function fit has been used for obtaining some observational characteristics of the energy-height relation, but now it is related to absolute reference level. The flattening point was defined as a place where the derivative of the fit is less than  $-145 \text{ km/keV}$ . This value has been chosen arbitrarily for defining qualitatively the point in which the observed relation changes from steep to flat (Fig. 1, right panel).

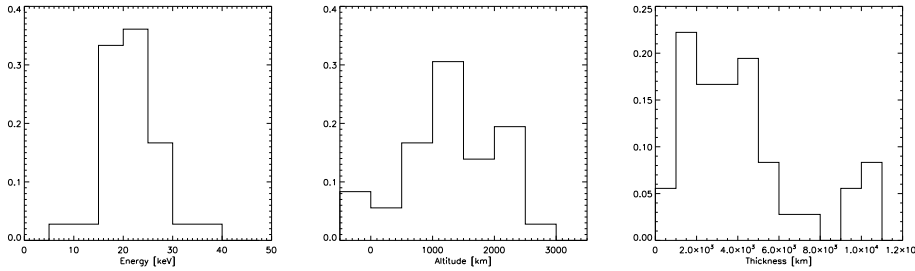


Figure 2: Histograms of the energy (left panel) and height above the photosphere (middle panel) of the flattening point and the centroid height range (right panel)

If we assume that the energy-height relation reflects the column density in a flux tube then the steep part is connected to low density region and the flat part occurs when density drastically rises.

The thickness of the region in which electrons deposit their energy due to Coulomb collisions (the collisional-stopping region) has been assumed as the difference between the maximal and the minimal altitude of centroid positions observed in each footpoint. The definition, based on centroids, of the collisional-stopping region gives a lower limit to the actual value because sources have a radial extent which is especially important at low energies.

### 3. Results

The observational characteristics of the analyzed energy-height relations are summarized in a form of normalized histograms (Fig. 2). The main findings are the following:

- The flattening point occurs in a relatively narrow energy interval. Almost all values fall within a 20–30 keV interval. According to the definition of the flattening point we can conclude that non-thermal HXR sources of energy 20–30 keV are markers of the location of a border between coronal plasma density and chromospheric plasma density.
- The obtained altitudes of the flattening point are consistent with existing models of the flaring chromosphere. Typical values are located in the range 1000–2500 km above the photosphere. The level of the

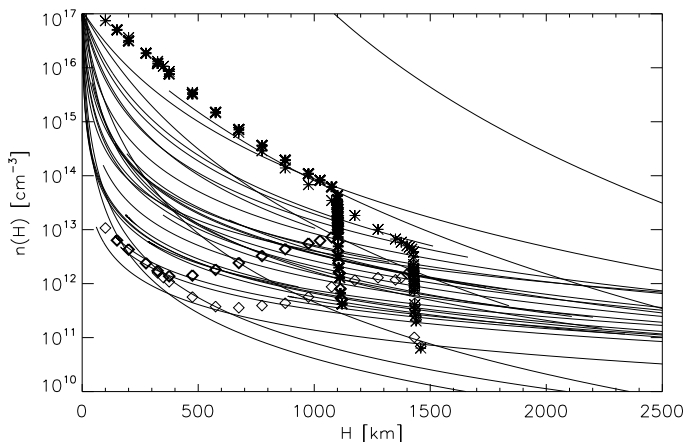


Figure 3: Density distribution in the collisional-stopping region estimated from observed energy-height relations. Semi-empirical models of flaring solar atmosphere (Machado et al. 1980) for bright (thick signs) and faint (thin signs) case. Neutral hydrogen density is marked with asterisks and electron density is marked with diamonds.

photosphere base was estimated with the use of the same data set. Thus, the obtained altitudes are much more reliable than the previous results obtained through comparison of observations from two or more different instruments.

- The thickness of the region in which a collisional stopping of non-thermal electrons took place is between 1000 km and 5000 km. This spread of values is connected mainly with the initial state (before an injection of non-thermal electrons) of the chromosphere. Lower values are observed mainly for the first bursts visible during the impulsive phase. Thickness obtained for the late stage of the impulsive phase are usually larger, up to 5000 km. The natural explanation of such behavior is occurrence of chromospheric evaporation.

With the use of the obtained energy-height relations we were able to derive the relation between the number density and a height measured above the base of the photosphere. The obtained values were compared to one of several existing solar atmosphere models (Fig. 3). Namely we chose semi-

empirical model of the flaring chromosphere calculated by Machado et al. (1980). Almost all of the density distributions derived from the observed energy-height relations fall within a region bounded by electron and neutral hydrogen densities from the model of Machado et al. (1980). This result shows that we can treat a non-thermal electron stream as a kind of tool probing chromospheric density.

It should be stressed that our analysis was based on a number of simplifying assumptions (neglected pitch-angle, no spectral dependence etc.). In the future we will include more parameters. Moreover, a detailed modelling of the energy-height relation is in progress.

#### 4. Acknowledgments

First, we wish to thank the *RHESSI* Team. We acknowledge many useful and inspiring discussions of Professor M. Tomczak. We also thank Barbara Cader-Sroka for valuable remarks that led to an improvement of this paper. This investigation has been supported by the Polish Ministry of Science and High Education, grant No. N203 1937 33.

#### References

- Aschwanden, M.J., Brown, J.C., Kontar, E.P.: 2002, *Solar Phys.* **210**, 383.  
Bogachev, S.A., Somov, B.V., Kosugi, T., Sakao, T.: 2005, *Astrophys. J.* **630**, 561.  
Brown, J.C., and McClymont, A.N.: 1975, *Solar Phys.* **41**, 135.  
Brown, J.C., Aschwanden, M.J., Kontar, E.P.: 2002, *Solar Phys.* **210**, 373.  
Högbom, J.A.: 1974, *A&A* **15**, 417.  
Hurford, G.J., Schmahl, E.J., Schwartz, R.A. et al.: 2002, *Solar Phys.* **210**, 61  
Lin, R.P., Dennis, B.R., Hurford, G.J. et al.: 2002, *Solar Phys.* **210**, 3  
Machado, M.E., Avrett, E.H., Vernazza, J.E., and Noyes, R.W.: 1980, *ApJ* **242**, 336  
Matsushita, K., Inada, M., Yaji, K.: 1992, *PASJ* **44**, L89.  
Mrozek, T.: 2006, *Adv. Space Res.* **38**, 962.  
Spitzer, L.W.: 1962, *Physics of Fully Ionized Gases*, 2nd ed., Interscience, New York